Interfacial cracks between piezoelectric and elastic materials under in-plane electric loading

M. Liu,   K.J. Hsia*

Department of Theoretical and Applied Mechanics,

University of Illinois at Urbana-Champaign,

Urbana, IL 61801

* Corresponding author. Tel.: +1-217-333-2321; fax: +1-217-244-5707.

E-mail: kj-hsia@uiuc.edu (K. J. Hsia)

Abstract

Evaluation of crack tip driving force for interfacial cracks between piezoelectric actuators and elastic substrates is crucial to successful applications of smart materials and smart structures. Here the behavior of an interfacial crack between a piezoelectric material and an elastic material under in-plane electric loading is studied. The displacement mismatch along a bonded interface due to electric potential loading on the piezoelectric material is modeled by an array of uniformly distributed dislocations along the interface. Using Fourier transformation method, the governing equations are converted to an integral equation, which is then converted to a standard Hilbert problem. A closed form solution for stresses, electric field, and electric displacements along the bonded interface is obtained. The results agree very well with that from numerical simulations using the finite element method. The results show that the closed form solution is not only accurate for far field distributions of stresses and electric variables, but also accurate for the asymptotic distributions near the crack tip. The solution also suggests the likelihood of domain switch in the piezoelectric material near the crack tip.

1. Introduction

Piezoelectric ceramics have recently been widely used in smart structures as electro-mechanical sensors and actuators (Ashley, 1995; Chopra, 1996). Since ceramic materials are brittle, fracture of piezoelectric ceramics has been a topic of extensive research. Researchers have developed linear (Pak, 1992; Sosa, 1992; Park and Sun, 1995a) and nonlinear theories (Yang and Suo, 1994; Gao et al., 1997; Zhu and Yang, 1999; Fotinich and Carman, 2000; Fulton and Gao, 2001) for fracture of piezoelectric ceramics. Experimental work has also been done to study fracture resistance and fracture mechanisms in piezoelectric materials (Park and Sun, 1995b; Heyer et al., 1998; Fu and Zhang, 2000; Busche and Hsia, 2001).

Interfacial fracture between piezoelectric actuators/sensors and elastic substrates presents an important concern in multilayer devices (Winzer et al., 1989; Furuta and Uchino, 1993; Kim and Jones, 1996), especially under mechanical and electric cyclic loading. Recent development of a new experimental technique by Du et al (2001) aims specifically at addressing this issue. However, evaluating the driving force at an interfacial crack tip between piezoelectric ceramics and substrate is a nontrivial task.

Most research to date has focused on the interfacial cracks between two different piezoelectric materials (Suo et al., 1992; Beom and Atluri, 1996; Shen et al., 1999; Gao and Wang, 2001). Cracks between piezoelectric actuators and elastic substrates are rarely studied, especially for in-plane, mode I/II cases. Narita and Shindo (1998) and Kwon and Lee (2000) solved the anti-plane (mode III) problem of an interfacial crack between a piezoelectric material and an elastic material. There exist a few analyses of the in-plane problem for interfacial cracks between piezoelectric materials and elastic materials (Parton, 1976; Ru, 2000; Govorukha and Loboda, 2000; Wang and Meguid, 2000). However, they are generally for special cases or under

mechanical loading. A solution for an interfacial crack between piezoelectric and elastic materials under in-plane electric loading does not exist.

In the present paper, the problem of an interfacial crack between a piezoelectric actuator and an elastic substrate under in-plane electric loading is studied. A semi-infinite piezoelectric medium bonded to a semi-infinite elastic medium along a segment of length $2a$ is considered. Following the approach used by Erdogan (1965) for interfacial cracks under thermal loading, electric field induced deformation mismatch between the piezoelectric medium and elastic medium is formulated by inserting an array of dislocations along the bonded interface. The approach used by Parton (1976) is employed to transform the governing partial differential equations into an integral equation, which is solved as a Hilbert problem. A closed-form solution for stresses, electric field, and electric displacements along the interface is obtained. The solution is compared with numerical simulation result using the finite element method. Excellent agreement between analytical and numerical solutions is achieved.

2. Problem Formulation

Here we consider two semi-infinite media occupying upper and lower half-planes, S^A and S^B, respectively (Fig.1a), with a piezoelectric material "A" in the upper plane and an elastic material "B" in the lower plane. The interface is located at $y = 0$ and the two materials are perfectly bonded along the interface on $-a \leq x \leq a$. The poling direction of the piezoelectric material "A" is along the positive y-axis. The electric potential φ is fixed to be zero along the interface and $-yE_0$ as $y \rightarrow +\infty$, so the average electric field in material "A" is always E_0.

The theory of piezoelectricity is briefly reviewed in Appendix A, in which x_1 denotes the x-direction and x_3 denotes the y-direction in Fig. 1. Under plane strain condition, the constitutive equations for the piezoelectric material (material "A") can be written as

4

$$\sigma_{xx}^{A} = C_{11}^{E} \frac{\partial u^{A}}{\partial x} + C_{13}^{E} \frac{\partial v^{A}}{\partial y} + e_{31} \frac{\partial \varphi^{A}}{\partial y},$$

$$\sigma_{yy}^{A} = C_{13}^{E} \frac{\partial u^{A}}{\partial x} + C_{33}^{E} \frac{\partial v^{A}}{\partial y} + e_{33} \frac{\partial \varphi^{A}}{\partial y},$$

$$\sigma_{xy}^{A} = C_{44}^{E} \left(\frac{\partial u^{A}}{\partial y} + \frac{\partial v^{A}}{\partial x} \right) + e_{15} \frac{\partial \varphi^{A}}{\partial x}, \tag{1}$$

$$D_{x}^{A} = e_{15} \left(\frac{\partial u^{A}}{\partial y} + \frac{\partial v^{A}}{\partial x} \right) - \in_{11}^{\varepsilon} \frac{\partial \varphi^{A}}{\partial x},$$

$$D_{y}^{A} = e_{31} \frac{\partial u^{A}}{\partial x} + e_{33} \frac{\partial v^{A}}{\partial y} - \in_{33}^{\varepsilon} \frac{\partial \varphi^{A}}{\partial y},$$

where u^{A}, v^{A} and φ^{A} are the displacements in the x-direction, y-direction and the electric potential, respectively. The superscript 'A' denotes the quantities in material "A". The physical meaning of material constants C^{E}, e and $\in^{\varepsilon}$ are explained in Appendix A.

Combining Eqs. (A1), (A4) and (A5), we can show that the equilibrium equations can then be expressed in terms of displacement components and electric potential as,

$$C_{11}^{E} \frac{\partial^{2} u^{A}}{\partial x^{2}} + C_{44}^{E} \frac{\partial^{2} u^{A}}{\partial y^{2}} + \left(C_{13}^{E} + C_{44}^{E} \right) \frac{\partial^{2} v^{A}}{\partial x \partial y} + \left(e_{31} + e_{15} \right) \frac{\partial^{2} \varphi^{A}}{\partial x \partial y} = 0$$

$$\left(C_{13}^{E} + C_{44}^{E} \right) \frac{\partial^{2} u^{A}}{\partial x \partial y} + C_{44}^{E} \frac{\partial^{2} v^{A}}{\partial x^{2}} + C_{33}^{E} \frac{\partial^{2} v^{A}}{\partial y^{2}} + e_{15} \frac{\partial^{2} \varphi^{A}}{\partial x^{2}} + e_{33} \frac{\partial^{2} \varphi^{A}}{\partial y^{2}} = 0 \tag{2}$$

$$\left(e_{31} + e_{15} \right) \frac{\partial^{2} u^{A}}{\partial x \partial y} + e_{15} \frac{\partial^{2} v^{A}}{\partial x^{2}} + e_{33} \frac{\partial^{2} v^{A}}{\partial y^{2}} - \in_{11}^{\varepsilon} \frac{\partial^{2} \varphi^{A}}{\partial x^{2}} - \in_{33}^{\varepsilon} \frac{\partial^{2} \varphi^{A}}{\partial y^{2}} = 0$$

Similarly, the constitutive law and the equilibrium equations for material "B" are

$$\sigma_{xx}^{B} = C_{11} \frac{\partial u^{B}}{\partial x} + C_{13} \frac{\partial v^{B}}{\partial y}$$

$$\sigma_{yy}^{B} = C_{13} \frac{\partial u^{B}}{\partial x} + C_{33} \frac{\partial v^{B}}{\partial y} \tag{3}$$

$$\sigma_{xy}^{B} = C_{44} \left(\frac{\partial u^{B}}{\partial y} + \frac{\partial v^{B}}{\partial x} \right)$$

$$C_{11}\frac{\partial^2 u^B}{\partial x^2} + C_{44}\frac{\partial^2 u^B}{\partial y^2} + \left(C_{13} + C_{44}\right)\frac{\partial^2 v^B}{\partial x \partial y} = 0$$

$$\left(C_{13} + C_{44}\right)\frac{\partial^2 u^B}{\partial x \partial y} + C_{44}\frac{\partial^2 v^B}{\partial x^2} + C_{33}\frac{\partial^2 v^B}{\partial y^2} = 0 \tag{4}$$

where, C_{11}, C_{13}, C_{33} and C_{44} are elastic constants for material "B".

Since Eqs. (1-4) are linear, we can apply the principle of superposition. The problem in Fig. 1a is equivalent to the superposition of two problems. The first is shown in Fig. 1b, where the upper and the lower half planes are not bonded, and the upper half plane is subjected to the same electric potential as that in Fig. 1a. The solution to this problem can be easily obtained as,

$$E_x^A = 0,\ E_y^A = E_0,\ D_x^A = 0,\ D_y^A = \in_{33}^\sigma E_0,$$
$$\varepsilon_{xx}^A(x,y) = d_{31}E_0,\ \varepsilon_{yy}^A(x,y) = d_{33}E_0,\ \varepsilon_{xy}^A(x,y) = 0,$$
$$\varepsilon_{xx}^B(x,y) = \varepsilon_{yy}^B(x,y) = \varepsilon_{xy}^B(x,y) = 0,$$
$$\sigma_{jk}^A(x,y) = \sigma_{jk}^B(x,y) = 0,\quad (j,k = x,y) \tag{5}$$

This solution has a strain discontinuity across the interface.

The second problem is illustrated in Fig. 1c, where the upper and lower planes are bonded along $-a \le x \le a$. To cancel the strain discontinuity caused by the piezoelectric strain under the applied electric field (Fig. 1b), an array of dislocations are uniformly placed along the interface. Therefore, the boundary conditions along the interface $(y = 0)$ are given as the following,

$$|x| \le a \qquad v^A(x,0) - v^B(x,0) = 0,\quad u^A(x,0) - u^B(x,0) = -d_{31}E_0 x \tag{6a}$$

$$|x| > a \qquad \sigma_{xy}^A(x,0) = \sigma_{xy}^B(x,0) = \sigma_{yy}^A(x,0) = \sigma_{yy}^B(x,0) = 0 \tag{6b}$$

$$|x| \le a \qquad \sigma_{xy}^A(x,0) = \sigma_{xy}^B(x,0),\quad \sigma_{yy}^A(x,0) = \sigma_{yy}^B(x,0) \tag{6c}$$

$$|x| < \infty \qquad \varphi^A(x,0) = 0 \tag{6d}$$

While, as $y \to \infty$, the far field boundary conditions are

$$u^A(x, y) = v^A(x, y) = u^B(x, y) = v^B(x, y) = \varphi^A(x, y) = 0 \tag{6e}$$

3. An Analytical Solution

To solve the problem posed in Fig. 1a, we firstly seek the solution to the problem posed in Fig. 1c. By using Fourier transformation method, we obtain the solutions to the governing Eqs. (2) and (4) in terms of 5 unknown functions. By applying the boundary conditions, the control equations of the unknown functions are derived and reduced to a singular integral equation, which can be solved as a standard Hilbert problem. The final solution of the problem in Fig. 1a can then be obtained by superposing this solution and that given by Eq. (5).

3.1 General forms of the solution

The piezoelectric material "A".

Using Fourier transformation, the displacements and electric potential in the piezoelectric material $(y \geq 0)$, can be expressed as

$$
\begin{aligned}
u^A(x, y) &= \sqrt{\frac{2}{\pi}} \int_0^\infty U^A(p, py) \sin(px) \mathrm{d}p, \\
v^A(x, y) &= \sqrt{\frac{2}{\pi}} \int_0^\infty V^A(p, py) \cos(px) \mathrm{d}p, \\
\varphi^A(x, y) &= \sqrt{\frac{2}{\pi}} \int_0^\infty \Phi^A(p, py) \cos(px) \mathrm{d}p.
\end{aligned}
\tag{7}
$$

where $U^A(p,py), V^A(p,py)$ and $\Phi^A(p,py)$ are the Fourier transforms of the displacements and the electric potential. These functions are referred to as kernel functions in the following. Substituting the above equations into Eq. (2), the equilibrium equations are reduced to a set of ordinary differential equations of the kernel functions,

$$C_{44}^E \frac{\mathrm{d}^2 U^A}{\mathrm{d}Y^2} - C_{11}^E U^A - \left(C_{13}^E + C_{44}^E\right)\frac{\mathrm{d}V^A}{\mathrm{d}Y} - \left(e_{31} + e_{15}\right)\frac{\mathrm{d}\Phi^A}{\mathrm{d}Y} = 0,$$

$$\left(C_{13}^E + C_{44}^E\right)\frac{\mathrm{d}U^A}{\mathrm{d}Y} + C_{33}^E \frac{\mathrm{d}^2 V^A}{\mathrm{d}Y^2} - C_{44}^E V^A + e_{33}\frac{\mathrm{d}^2 \Phi^A}{\mathrm{d}Y^2} - e_{15}\Phi^A = 0, \qquad (8)$$

$$\left(e_{31} + e_{15}\right)\frac{\mathrm{d}U^A}{\mathrm{d}Y} + e_{33}\frac{\mathrm{d}^2 V^A}{\mathrm{d}Y^2} - e_{15}V^A - \in_{33}^\varepsilon \frac{\mathrm{d}^2 \Phi^A}{\mathrm{d}Y^2} + \in_{11}^\varepsilon \Phi^A = 0.$$

where $Y = py$.

The solution to the above differential equations can be expressed in the following form (See Appendix B),

$$\begin{bmatrix} U^A(p, py) \\ V^A(p, py) \\ \Phi^A(p, py) \end{bmatrix} = \begin{Bmatrix} \alpha_1^A \\ \beta_1^A \\ \gamma_1^A \end{Bmatrix} L^A(p)e^{-\kappa_1^A py} + \mathrm{Re}\left(\begin{Bmatrix} \alpha_2^A \\ \beta_2^A \\ \gamma_2^A \end{Bmatrix} M^A(p)e^{-\kappa_2^A py} \right) \qquad (9)$$

where $L^A(p)$ is a real function and $M^A(p)$ is a complex function to be determined from the boundary conditions. The real coefficients $\alpha_1^A, \beta_1^A, \gamma_1^A, \ \kappa_1^A$ and the complex coefficients $\alpha_2^A, \beta_2^A, \gamma_2^A, \ \kappa_2^A$ are functions of the material properties, which are obtained by solving an eigenvalue problem (Appendix B).

The elastic material "B".

Similarly, using the first two Fourier transforms in Eq. (7), the equilibrium equations for the elastic material $(y \leq 0)$ can be reduced to two ordinary differential equations of the kernel functions $U^B(p, py)$ and $V^B(p, py)$,

$$C_{44}\frac{\mathrm{d}^2 U^B}{\mathrm{d}Y^2} - C_{11}U^B - \left(C_{13} + C_{44}\right)\frac{\mathrm{d}V^B}{\mathrm{d}Y} = 0$$

$$\left(C_{13} + C_{44}\right)\frac{\mathrm{d}U^B}{\mathrm{d}Y} + C_{33}\frac{\mathrm{d}^2 V^B}{\mathrm{d}Y^2} - C_{44}V^B = 0 \qquad (10)$$

For isotropic materials $\lambda = C_{13}, \mu = C_{44}$, where λ and μ are the Lamé constants, the kernel functions can then be determined as (See Appendix C),

8

$$\begin{Bmatrix} U^B(p,py) \\ V^B(p,py) \end{Bmatrix} = \begin{Bmatrix} L^B(p) \\ -L^B(p) + \dfrac{\lambda+3\mu}{\lambda+\mu}M^B(p) \end{Bmatrix} e^{py} + \begin{Bmatrix} M^B(p) \\ -M^B(p) \end{Bmatrix} pye^{py} \tag{11}$$

where $L^B(p)$ and $M^B(p)$ are real functions.

3.2. Interfacial boundary conditions

Combining Eqs. (1,3,7,9,11), we show that quantities along the interface $(y=0)$ can be expressed as the following,

$$u^A(x,0) = \sqrt{\frac{2}{\pi}} \int_0^\infty \left[\alpha_1^A L^A(p) + \mathrm{Re}\left\{ \alpha_2^A M^A(p) \right\} \right] \sin(px)\,\mathrm{d}p \tag{12a}$$

$$v^A(x,0) = \sqrt{\frac{2}{\pi}} \int_0^\infty \left[\beta_1^A L^A(p) + \mathrm{Re}\left\{ \beta_2^A M^A(p) \right\} \right] \cos(px)\,\mathrm{d}p \tag{12b}$$

$$\varphi^A(x,0) = \sqrt{\frac{2}{\pi}} \int_0^\infty \left[\gamma_1^A L^A(p) + \mathrm{Re}\left\{ \gamma_2^A M^A(p) \right\} \right] \cos(px)\,\mathrm{d}p \tag{12c}$$

$$\frac{\partial \varphi^A(x,0)}{\partial y} = \sqrt{\frac{2}{\pi}} \int_0^\infty \left[-\kappa_1^A \gamma_1^A L^A(p) - \mathrm{Re}\left\{ \kappa_2^A \gamma_2^A M^A(p) \right\} \right] p\cos(px)\,\mathrm{d}p \tag{12d}$$

$$\sigma_{xy}{}^A(x,0) = \sqrt{\frac{2}{\pi}} \int_0^\infty \left[Q_1 L^A(p) + \mathrm{Re}\left\{ Q_2 M^A(p) \right\} \right] p\sin(px)\,\mathrm{d}p \tag{12e}$$

$$\sigma_{yy}{}^A(x,0) = \sqrt{\frac{2}{\pi}} \int_0^\infty \left[P_1 L^A(p) + \mathrm{Re}\left\{ P_2 M^A(p) \right\} \right] p\cos(px)\,\mathrm{d}p \tag{12f}$$

$$u^B(x,0) = \sqrt{\frac{2}{\pi}} \int_0^\infty L^B(p)\sin(px)\,\mathrm{d}p \tag{12g}$$

$$v^B(x,0) = \sqrt{\frac{2}{\pi}} \int_0^\infty \left[-L^B(p) + \frac{\lambda+3\mu}{\lambda+\mu}M^B(p) \right] \cos(px)\,\mathrm{d}p \tag{12h}$$

$$\sigma_{xy}{}^B(x,0) = \sqrt{\frac{2}{\pi}} \int_0^\infty \left[2\mu L^B(p) - 2\mu \frac{\mu}{\lambda+\mu}M^B(p) \right] p\sin(px)\,\mathrm{d}p \tag{12i}$$

9

$$\sigma_{yy}{}^{B}(x,0) = \sqrt{\frac{2}{\pi}} \int_0^{\infty} \left[-2\mu L^{B}(p) + 2\mu \frac{\lambda+2\mu}{\lambda+\mu} M^{B}(p) \right] p\cos(px)\,\mathrm{d}p \qquad (12j)$$

where Q_1, P_1 are real numbers and Q_2, P_2 are complex numbers, given as

$$Q_1 = -C_{44}^{E}\left(\alpha_1^{A}\kappa_1^{A} + \beta_1^{A}\right) - e_{15}\gamma_1^{A}, \qquad Q_2 = -C_{44}^{E}\left(\alpha_2^{A}\kappa_2^{A} + \beta_2^{A}\right) - e_{15}\gamma_2^{A},$$

$$P_1 = C_{13}^{E}\alpha_1^{A} - C_{33}^{E}\kappa_1^{A}\beta_1^{A} - e_{33}\kappa_1^{A}\gamma_1^{A} \qquad P_2 = C_{13}^{E}\alpha_2^{A} - C_{33}^{E}\kappa_2^{A}\beta_2^{A} - e_{33}\kappa_2^{A}\gamma_2^{A}$$

It should be clear that P_1, Q_1, P_2, and Q_2 are constants related to material constants alone. The only unknown variables are the five real functions $L^{A}(p)$, $L^{B}(p)$, $\mathrm{Re}(M^{A}(p))$, $\mathrm{Im}(M^{A}(p))$, and $M^{B}(p)$.

In most research work to date (Narita and Shindo, 1998; Kwon and Lee, 2000; Wang and Meguid, 2000), a uniform electric field or an electric displacement is applied to the piezoelectric medium instead of electric potentials. This simplifies the problem significantly. It can be proved that for mode III case (Narita and Shindo, 1998; Kwon and Lee, 2000), an application of a uniform electric field is equivalent to an application of an electric potential because of the uncoupled governing equations. However, this is not the case for the in-plane problem studied here. A uniform electric field loading can be easily implemented by letting Eq. (12d) equal to zero. In the present study, however, only the electric potential loading is considered since it is the case in experimental studies (Park and Sun, 1995b; Heyer et al., 1998; Fu and Zhang, 2000; Du et al., 2001)

By applying the boundary conditions in Eqs. (6b-d), it can be shown that only two of the five unknown functions are linearly independent. If we select $L^{A}(p)$ and $\mathrm{Re}\{M^{A}(p)\}$ as the independent functions, the others can be expressed in the following,

$$\text{Im}\{M^A(p)\} = \frac{1}{\text{Im}\{\gamma_2\}}\left[\gamma_1 L^A(p) + \text{Re}\{\gamma_2\}\text{Re}\{M^A(p)\}\right]$$

$$\begin{Bmatrix} L^B(p) \\ M^B(p) \end{Bmatrix} = \frac{1}{2\mu}\begin{bmatrix} \dfrac{\lambda+2\mu}{\lambda+\mu}\delta_1 + \dfrac{\mu}{\lambda+\mu}\delta_3 & \dfrac{\lambda+2\mu}{\lambda+\mu}\delta_2 + \dfrac{\mu}{\lambda+\mu}\delta_4 \\ \delta_1 + \delta_3 & \delta_2 + \delta_4 \end{bmatrix}\begin{Bmatrix} L^A(p) \\ \text{Re}\{M^A(p)\} \end{Bmatrix} \qquad (13)$$

Furthermore, boundary conditions (6a,b) require that $L^A(p)$ and $\text{Re}\{M^A(p)\}$ must satisfy the following integral equations along the interface $(y = 0)$,

$$\begin{cases} \sigma_{xy}(x, 0) = \sqrt{\dfrac{2}{\pi}}\displaystyle\int_0^\infty \left[\delta_1 L^A(p) + \delta_2\,\text{Re}\{M^A(p)\}\right]p\sin(px)\mathrm{d}p = 0 \\[4mm] \sigma_{yy}(x, 0) = \sqrt{\dfrac{2}{\pi}}\displaystyle\int_0^\infty \left[\delta_3 L^A(p) + \delta_4\,\text{Re}\{M^A(p)\}\right]p\cos(px)\mathrm{d}p = 0 \end{cases} \qquad |x| > a \quad (14a)$$

$$\begin{cases} \dfrac{\mathrm{d}(v^A - v^B)}{\mathrm{d}x} = \sqrt{\dfrac{2}{\pi}}\displaystyle\int_0^\infty \left[\delta_5 L^A(p) + \delta_6\,\text{Re}\{M^A(p)\}\right]p\sin(px)\mathrm{d}p = 0 \\[4mm] \dfrac{\mathrm{d}(u^A - u^B)}{\mathrm{d}x} = \sqrt{\dfrac{2}{\pi}}\displaystyle\int_0^\infty \left[\delta_7 L^A(p) + \delta_8\,\text{Re}\{M^A(p)\}\right]p\cos(px)\mathrm{d}p = -d_{31}E_0 \end{cases} \qquad |x| \le a \quad (14b)$$

where, δ_j, $(j = 1-8)$ are constants and given in Appendix D.

3.3. The solution

Define a complex stress function $f(x)$ as

$$f(x) = \sigma_{yy}(x, 0) + ig_0\sigma_{xy}(x, 0) \qquad (15)$$

where $i = \sqrt{-1}$. We can then rewrite Eqs. (14a) and (14b) into a single, governing integral equation (See Appendix E),

$$f(x) + g\frac{1}{\pi i}\int_{-a}^a \frac{f(t)\mathrm{d}t}{t - x} = \frac{d_{31}E_0}{g_1} \qquad (16)$$

where g, g_0 and g_1 are constants determined from the material properties given in Appendix E.

To solve Eq. (16), we define a complex function of complex variable $z = x + iy$, given as,

$$F(z) = \frac{1}{2\pi i} \int_{-a}^{a} \frac{f(t)}{t-z} dt \tag{17}$$

$F(z)$ is analytic in the whole plane except for $-a \le x \le a$, $y = 0$.

Using the Sokhotski-Plemelj formulae,

$$F^+(x) = \frac{1}{2}f(x) + \frac{1}{2\pi i}\int_{-a}^{a}\frac{f(t)}{t-x}dt, \quad F^-(x) = -\frac{1}{2}f(x) + \frac{1}{2\pi i}\int_{-a}^{a}\frac{f(t)}{t-x}dt \tag{18}$$

Equation (16) can be converted into a standard Hilbert problem, given as

$$F^+(x) = -\frac{g-1}{g+1}F^-(x) + \frac{d_{31}E_0}{g_1(g+1)} \tag{19}$$

where the '+' and '-' signs denote the limiting values of $F(z)$ at $y = 0$ from the positive and negative y-axis, respectively.

For real materials, $g > 1$, therefore $-\frac{g-1}{g+1} < 0$. The solution to Eq. (19) can then be obtained as the following (Muskhelishvili, 1953),

$$F(z) = \frac{X(z)}{2\pi i}\int_{-a}^{a}\frac{d_{31}E_0}{g_1(g+1)}\frac{1}{(t-z)X^+(x)}dt + c_0 X(z) \tag{20}$$

where $X(z)$ is the solution for the homogeneous Hilbert problem, given as

$$X(z) = (z+a)^{-\frac{1}{2}+i\eta}(z-a)^{-\frac{1}{2}-i\eta} \tag{21}$$

where $\eta = \frac{1}{2\pi}\log\left(\frac{g-1}{g+1}\right)$ is a parameter related to the elastic and piezoelectric properties of the two materials. In Eq. (21), the branch $\lim_{z \to \infty} z\, X(z) = 1$ of $X(z)$ is taken.

Since there is no net external forces applied to the body, $c_0 = 0$ (Erdogan, 1965). The solution to Eq. (19) is then

$$F(z) = \frac{d_{31}E_0}{2gg_1}\left[1 - (z - i2a\eta)X(z)\right] \tag{22}$$

Using the Sokhotski-Plemelj formulae, the stresses along the bonded interface $(y = 0, |x| \le a)$

can be obtained as

$$\sigma_{yy}(x,0) = \frac{Q_0}{\sqrt{a^2 - x^2}}\left[-2a\eta\cos\left(\eta\log\frac{a-x}{a+x}\right) - x\sin\left(\eta\log\frac{a-x}{a+x}\right)\right]$$

$$\tag{23}$$

$$\sigma_{xy}(x,0) = \frac{Q_0}{g_0\sqrt{a^2 - x^2}}\left[-x\cos\left(\eta\log\frac{a-x}{a+x}\right) + 2a\eta\sin\left(\eta\log\frac{a-x}{a+x}\right)\right]$$

where $Q_0 = \dfrac{d_{31}E_0}{g_1\sqrt{g^2 - 1}}$.

Substituting Eq. (23) into Eqs. (E1-E3) and using Eqs. (1,7,9,13,18), the electric variables

can then be obtained as

$$E_y(x,0) = \frac{Q_0}{\sqrt{a^2 - x^2}}\left(\frac{q_1}{gg_0} - q_2\right)\left[2a\eta\cos\left(\eta\log\frac{a-x}{a+x}\right) + x\sin\left(\eta\log\frac{a-x}{a+x}\right)\right]$$

$$- \frac{Q_0 q_1\sqrt{g^2 - 1}}{gg_0} \tag{24}$$

$$D_x(x,0) = \frac{Q_0}{\sqrt{a^2 - x^2}}\left(\frac{q_3}{g_0} + \frac{q_4}{g}\right)\left[-x\cos\left(\eta\log\frac{a-x}{a+x}\right) + 2a\eta\sin\left(\eta\log\frac{a-x}{a+x}\right)\right]$$

$$\tag{25}$$

$$D_y(x,0) = \frac{Q_0}{\sqrt{a^2 - x^2}}\left(\frac{q_5}{gg_0} - q_6\right)\left[2a\eta\cos\left(\eta\log\frac{a-x}{a+x}\right) + x\sin\left(\eta\log\frac{a-x}{a+x}\right)\right]$$

$$- Q_0\frac{q_5\sqrt{g^2 - 1}}{gg_0}$$

where q_j, $(j = 1-6)$ are constants given in Appendix D.

3.4 Superposition of the solutions

Equations (23-25) give the solution to the problem posed in Fig. 1c. The solution to the problem illustrated in Fig. 1b is given in Eq. (5). Therefore, the complete solution to the problem posed in Fig. 1a can be obtained by simply superposing the uniform electric field $E_y = E_0$ and electric displacement $D_y = \in_{33}^{\sigma} E_0$ onto Eqs. (24) and (25) respectively. It is seen that, near the crack tip, the solution is dominated by the singular term; whereas far away from the crack tip, the uniform field prevails.

4. Results and Discussion

The solution obtained in the previous section can be used to evaluate the distributions of the stresses, electric displacements, and electric field along the bonded interface between the piezoelectric material and elastic material. To be consistent with our experimental study (Du et al., 2001), here we choose a PZT ceramic as the piezoelectric material and aluminum as the elastic material. The elastic and piezoelectric constants for these two materials are listed in Table 1.

Furthermore, numerical results are obtained using the commercial finite element package ANSYS5.7. Due to symmetry, only half of the configuration is considered in the simulation. The geometry and the finite element mesh used in the computation are shown in Figs. 2a-b. About 7000 four-node elements are used in the simulation. The size of the smallest element at the crack tip is about 5×10^{-5} of the half length of bonded region, a. To simulate an infinite body, we choose $w/a = 100$, $h/a = 20$. To determine whether the configuration is sufficiently large to approximate an infinite body, a case of $w/a = 20$ is also computed. The differences in all variables between the two cases are always less than one percent. In the calculations, the bottom boundary of PZT has a fixed potential of $\varphi = 0$, and the top boundary is electrically loaded to a potential of $\varphi = 100 \, \text{kV}$, which results in an average field of $E_0 = 10 \, \text{kV}/\text{cm}$ (with $w = 10 \text{cm}$).

Results of the normal and shear stresses along the bonded interface are plotted in Figs. 3a and 3b. The solid line is the analytic solution, Eq. (23), and the dots are the numerical simulation result. Figures. 3a and 3b show that excellent agreement between the analytical solution and numerical simulation is reached not only in the far field away from the crack tip, but also in the vicinity of the crack tip. Moreover, these stress distributions exhibit very similar trend as that of shear force transfer between fibers and matrix in a fiber-reinforced composite material, a phenomenon well documented in literature (see, for example, Carrara and McGarry, 1968; Broutman and Agarwal, 1974).

From the analytical solution, the asymptotic stress distributions near the crack tip can be expressed in terms of the distance from the crack, $r = a - x$, as,

$$\sigma_{yy}(r,0) = \frac{1}{\sqrt{2\pi r}} \mathrm{Re}\left\{ \boldsymbol{K}\left(\frac{r}{2a}\right)^{i\eta} \right\}, \quad \sigma_{xy}(r,0) = -\frac{1}{g_0}\frac{1}{\sqrt{2\pi r}} \mathrm{Im}\left\{ \boldsymbol{K}\left(\frac{r}{2a}\right)^{i\eta} \right\} \quad (26)$$

where the complex stress intensity factor

$$\boldsymbol{K} = K_1 + iK_2 = -Q_0\sqrt{\pi a}\left(2\eta - i\right). \tag{27}$$

It is not surprising that, like all asymptotic solutions of a crack between two dissimilar elastic media, this asymptotic field has a $\frac{1}{\sqrt{r}}$ singularity and an oscillatory term, $\left(\frac{r}{2a}\right)^{i\eta}$. For a crack between two different, isotropic elastic materials, Rice (1988) obtained an expression of asymptotic stress distribution, as

$$\sigma_{yy} = \frac{1}{\sqrt{2\pi r}} \mathrm{Re}\left\{(K_1 + iK_2)r^{i\eta}\right\}, \quad \sigma_{xy} = \frac{1}{\sqrt{2\pi r}} \mathrm{Im}\left\{(K_1 + iK_2)r^{i\eta}\right\} \tag{28}$$

Compare Eqs. (26) and (28), it is noted that the expressions differ from each other by a factor of $-\frac{1}{g_0}$ for the shear stress distribution, where g_0, given in Appendix E, is related to the

15

piezoelectric and elastic properties of the two materials. Furthermore, the oscillatory term in Eq. (26) is non-dimensionalized, whereas the oscillatory term $r^{i\eta}$ in Eq. (28) is dependent on the unit with which r is measured. It is also noted that in plotting Figs. 3a and 3b, the data points closest to the crack tip are at a distance $\dfrac{r}{a} \approx 2 \times 10^{-4}$ from the crack tip. At this distance from the crack tip, no oscillatory behavior is visible either in the numerical solution or in the analytical solution. For a bonded length of $a = 5$mm, this distance represents a point about 1μm from the crack tip, which is well within the region where local microstructure of the material may affect the stress distributions. Therefore, the oscillatory behavior within about 1μm from the crack tip is unimportant.

The results for the electric field and electric displacements are plotted in Fig. 4, Figs. 5a and 5b, respectively. The figures show that, although the magnitude of D_x increases rapidly near the crack tip in a similar manner as the singular behavior of the stresses, the magnitudes of E_y and D_y decrease near the crack tip because of the prescribed boundary conditions. Reaching a critical electric displacement has been proposed as a criterion for domain switch (Fotinich and Carman, 2000). Due to the rapidly increasing nature of D_x and decreasing of D_y near the crack tip, 90°-domain switch from the poling direction (*y*-direction) to the direction parallel to the crack is likely to happen. Such 90°-domain switch will then affect the stress distribution near the crack tip (Zhu and Yang, 1999; Busche and Hsia, 2001), which will in turn affect the fracture resistance of interface.

5. Conclusion

In this paper, the behavior of an interfacial crack between a semi-infinite elastic material and a semi-infinite piezoelectric material under in-plane electric potential loading is studied. Using

Fourier transformation, the governing equations are reduced to an integral equation, which is then converted to a standard Hilbert problem. A closed-form solution for stresses, electric field and electric displacements is obtained. The results of stress, electric field, and electric displacement distributions along the bonded interface are presented. The results agree very well with that of numerical simulations using the finite element method.

The results indicate that, unlike in the anti-plane case (Narita and Shindo, 1998; Kwon and Lee, 2000), the solution for prescribed electric potential at the boundary and that for prescribed uniform electric field throughout the piezoelectric material are different, primarily due to the coupling of in-plane variables. Such coupling makes the problem significantly more complex. The solution obtained in this paper is the full field solution, applicable not only to regions far away from the crack tip but also to the near tip region. The asymptotic distributions of stresses, electric field, and electric displacements show an oscillatory singularity similar to that for interfacial cracks between two different elastic media, albeit additional factors specific to the piezoelectric properties of the material are present. The normal and shear stress distributions along the bonded interface resemble that of the shear force transfer between fiber and matrix in fiber-reinforced composites. While the electric displacement component parallel to the crack exhibits singular increase near the crack tip, electric field and electric displacement component perpendicular to the crack decrease in magnitude near the crack tip. Such distributions will likely give rise to 90°-domain switch of the piezoelectric material in the near tip region, thus altering the crack tip stress distribution as well as fracture resistance. This problem can only be addressed using nonlinear analysis, which is beyond the scope of the current work.

Acknowledgement

Appendix A

Most poled piezoelectric ceramics exhibit transversely isotropic elastic behavior with hexagonal symmetry with x_3 as the poling direction and $x_1 - x_2$ plane as the isotropic plane (Pak, 1992). The constitutive equations for such piezoelectric materials can be written as

$$\boldsymbol{\sigma} = \boldsymbol{C}^E \boldsymbol{\varepsilon} - \boldsymbol{e}^{\mathrm{T}} \boldsymbol{E}$$
$$\boldsymbol{D} = \boldsymbol{e}\,\boldsymbol{\varepsilon} + \boldsymbol{\epsilon}^{\varepsilon}\,\boldsymbol{E} \tag{A1}$$

where the superscript 'T' stands for the transpose of a vector or a matrix and

$$\boldsymbol{\sigma} = \{\sigma_{11}\ \ \sigma_{22}\ \ \sigma_{33}\ \ \sigma_{32}\ \ \sigma_{31}\ \ \sigma_{12}\}^{\mathrm{T}}, \ \ \boldsymbol{\varepsilon} = \{\varepsilon_{11}\ \ \varepsilon_{22}\ \ \varepsilon_{33}\ \ 2\varepsilon_{32}\ \ 2\varepsilon_{31}\ \ 2\varepsilon_{12}\}^{\mathrm{T}}, \ \ \boldsymbol{D} = \{D_1\ \ D_2\ \ D_3\}^{\mathrm{T}}$$

and $\boldsymbol{E} = \{E_1\ \ E_2\ \ E_3\}^{\mathrm{T}}$ stand for the stress, strain, electric displacement and electric field vectors, respectively. $\boldsymbol{C}^E$, $\boldsymbol{e}$ and $\boldsymbol{\epsilon}^{\varepsilon}$ denote the stiffness matrix measured at zero electric field, the piezoelectric stress constant matrix and the dielectric constant matrix measured at zero strain, respectively. They can be written in the following forms,

$$\boldsymbol{C}^E = \begin{Bmatrix} C_{11}^E & C_{12}^E & C_{13}^E & 0 & 0 & 0 \\ C_{12}^E & C_{11}^E & C_{13}^E & 0 & 0 & 0 \\ C_{13}^E & C_{13}^E & C_{33}^E & 0 & 0 & 0 \\ 0 & 0 & 0 & C_{44}^E & 0 & 0 \\ 0 & 0 & 0 & 0 & C_{44}^E & 0 \\ 0 & 0 & 0 & 0 & 0 & \frac{1}{2}\left(C_{11}^E - C_{12}^E\right) \end{Bmatrix},$$

$$\boldsymbol{e} = \begin{Bmatrix} 0 & 0 & 0 & 0 & e_{15} & 0 \\ 0 & 0 & 0 & e_{15} & 0 & 0 \\ e_{31} & e_{31} & e_{33} & 0 & 0 & 0 \end{Bmatrix}, \ \ \boldsymbol{\epsilon}^{\varepsilon} = \begin{Bmatrix} \epsilon_{11}^{\varepsilon} & 0 & 0 \\ 0 & \epsilon_{11}^{\varepsilon} & 0 \\ 0 & 0 & \epsilon_{33}^{\varepsilon} \end{Bmatrix}$$

The constitutive equations can be expressed in another form, which is

$$\boldsymbol{\varepsilon} = \boldsymbol{S}^E \boldsymbol{\sigma} + \boldsymbol{d}^{\mathrm{T}} \boldsymbol{E}$$
$$\boldsymbol{D} = \boldsymbol{d}\boldsymbol{\sigma} + \boldsymbol{\epsilon}^{\sigma}\,\boldsymbol{E} \tag{A2}$$

18

where S^E, d and ϵ^σ denote the compliance matrix measured at zero electric field, piezoelectric strain constant matrix and dielectric constant matrix measured at zero stress, respectively. They are related to C^E, e and ϵ^ε as the following,

$$S^E = \left(C^E\right)^{-1}, \quad d = eS^E, \quad \epsilon^\sigma = \epsilon^\varepsilon + ed^T \tag{A3}$$

The strain-displacement and the electric field-electric potential relations can be written as

$$\varepsilon_{jk} = \frac{1}{2}\left(\frac{\partial u_j}{\partial x_k} + \frac{\partial u_k}{\partial x_j}\right), \quad E_j = -\frac{\partial \varphi}{\partial x_j} \quad (j, k = 1, 2, 3) \tag{A4}$$

where u_j and φ are the displacement components and electric potential respectively.

If there are no body force and body charge, the equilibrium equations can be written as

$$\sigma_{jk,k} = 0, \quad D_{j,j} = 0 \quad (j, k = 1, 2, 3) \tag{A5}$$

Appendix B

The solution of Eq. (8) has the form of

$$U^A = \alpha^A e^{-\kappa^A Y}, \quad V^A = \beta^A e^{-\kappa^A Y}, \quad \Phi = \gamma^A e^{-\kappa^A Y} \tag{B1}$$

where α^A, β^A, γ^A and κ^A satisfy the following eigenvalue problem,

$$\begin{bmatrix} a_{11} & a_{12} & a_{13} \\ -a_{12} & a_{22} & a_{23} \\ -a_{13} & a_{23} & a_{33} \end{bmatrix} \begin{Bmatrix} \alpha^A \\ \beta^A \\ \gamma^A \end{Bmatrix} = \begin{Bmatrix} 0 \\ 0 \\ 0 \end{Bmatrix} \tag{B2}$$

in which

$$a_{11} = C_{44}^E\left(\kappa^A\right)^2 - C_{11}^E, \quad a_{12} = \left(C_{13}^E + C_{44}^E\right)\kappa^A, \quad a_{13} = \left(e_{31} + e_{15}\right)\kappa^A,$$
$$a_{22} = C_{33}^E\left(\kappa^A\right)^2 - C_{44}^E, \quad a_{23} = e_{33}\left(\kappa^A\right)^2 - e_{15}, \quad a_{33} = -\epsilon_{33}^\varepsilon\left(\kappa^A\right)^2 + \epsilon_{11}^\varepsilon \tag{B3}$$

For a non-trivial solution to exist, the coefficient matrix of Eq. (B2) must satisfy $\det\left|a_{jk}\right| = 0$. In case of real piezoelectric materials, κ^A has six different roots, $\pm\zeta$ and

$\pm(\delta \pm i\omega)$, where ζ, δ and ω are positive real numbers. For future convenience, we denote them as $\kappa_j^A, (j = 1-6)$, which are given by

$$
\begin{aligned}
&\kappa_1^A = \zeta,\ \kappa_2^A = \delta + i\omega,\ \kappa_3^A = \delta - i\omega, \\
&\kappa_4^A = -\zeta,\ \kappa_5^A = -(\delta + i\omega),\ \kappa_6^A = -(\delta - i\omega)
\end{aligned}
\tag{B4}
$$

To simplify the derivation of the kernels, we define three functions in the following

$$
\Theta_1(\kappa^A) = a_{12}a_{23} - a_{13}a_{22},\ \ \Theta_2(\kappa^A) = -a_{11}a_{23} - a_{12}a_{13},\ \ \Theta_3(\kappa^A) = a_{11}a_{22} + a_{12}^2. \tag{B5}
$$

When $y \to \infty$, all the field variables approach zero, Eq. (6e). As a result, only κ_j^A

$(j = 1, 2, 3)$ that have positive real part need to be considered. Therefore, by letting

$$
\alpha_j^A = \Theta_1(\kappa_j^A),\ \ \beta_j^A = \Theta_2(\kappa_j^A),\ \ \gamma_j^A = \Theta_3(\kappa_j^A),\ \ (j = 1, 2) \tag{B6}
$$

the kernel functions can be expressed as Eq. (9).

Appendix C

By letting $U^B = \alpha^B e^{-\kappa^B Y}, V^B = \beta^B e^{-\kappa^B Y}$, differential equations, Eq. (10), become

$$
\begin{bmatrix} C_{44}(\kappa^B)^2 - C_{11} & (C_{13} + C_{44})\kappa^B \\ -(C_{13} + C_{44})\kappa^B & C_{33}(\kappa^B)^2 - C_{44} \end{bmatrix} \begin{Bmatrix} \alpha^B \\ \beta^B \end{Bmatrix} = \begin{Bmatrix} 0 \\ 0 \end{Bmatrix} \tag{C1}
$$

The non-trivial solution requires the determinant of the coefficient matrix to be zero. For real anisotropic materials, this requirement leads to two pairs of conjugate complex roots, $\kappa_j^B = \pm(\delta \pm i\omega), (j = 1-4)$. For isotropic materials, however, this requirement will lead to two double roots $\kappa_{1,2}^B = 1$ and $\kappa_{3,4}^B = -1$. In this paper, the attentions will be focused on the isotropic materials, but it should be noted that there is no difficulty in applying this method to anisotropic materials.

Since the elastic plane is below *x*-axis, the vanishing far field boundary condition requires that $\kappa_{3,4}^B = -1$ should be used. Noted that $\kappa_{3,4}^B = -1$ is a double root, the solutions of U^B and V^B are in the form of

$$U^B = \Lambda_1(p)e^Y + \Lambda_2(p)Y e^Y$$
$$V^B = \Lambda_3(p)e^Y + \Lambda_4(p)Y e^Y$$

(C2)

where $\Lambda_j(p), (j = 1-4)$ are arbitrary real functions. Substituting (C2) into Eq. (10) and rewriting $\Lambda_1(p), \Lambda_2(p)$ as $L^B(p), M^B(p)$ respectively, the kernel functions can then be determined as Eq. (11).

Appendix D

Constants for Eq. (13) and (14a,b),

$$\delta_1 = Q_1 + \frac{\gamma_1^A}{\text{Im}\{\gamma_2^A\}}\text{Im}\{Q_2\}, \qquad \delta_2 = \text{Re}\{Q_2\} + \frac{\text{Re}\{\gamma_2^A\}}{\text{Im}\{\gamma_2^A\}}\text{Im}\{Q_2\},$$

$$\delta_3 = P_1 + \frac{\gamma_1^A}{\text{Im}\{\gamma_2^A\}}\text{Im}\{P_2\}, \qquad \delta_4 = \text{Re}\{P_2\} + \frac{\text{Re}\{\gamma_2^A\}}{\text{Im}\{\gamma_2^A\}}\text{Im}\{P_2\}.$$

$$\delta_5 = \beta_1^A - \frac{\gamma_1^A}{\text{Im}\{\gamma_2^A\}}\text{Im}\{\beta_2^A\} - \frac{\delta_1}{2(\lambda+\mu)} - \frac{(\lambda+2\mu)\delta_3}{2\mu(\lambda+\mu)},$$

$$\delta_6 = \text{Re}\{\beta_2^A\} - \frac{\text{Re}\{\gamma_2^A\}}{\text{Im}\{\gamma_2^A\}}\text{Im}\{\beta_2^A\} - \frac{\delta_2}{2(\lambda+\mu)} - \frac{(\lambda+2\mu)\delta_4}{2\mu(\lambda+\mu)}$$

$$\delta_7 = \alpha_1^A - \frac{\gamma_1^A}{\text{Im}\{\gamma_2^A\}}\text{Im}\{\alpha_2^A\} - \frac{\delta_3}{2(\lambda+\mu)} - \frac{(\lambda+2\mu)\delta_1}{2\mu(\lambda+\mu)},$$

$$\delta_8 = \text{Re}\{\alpha_2^A\} - \frac{\text{Re}\{\gamma_2^A\}}{\text{Im}\{\gamma_2^A\}}\text{Im}\{\alpha_2^A\} - \frac{\delta_4}{2(\lambda+\mu)} - \frac{(\lambda+2\mu)\delta_2}{2\mu(\lambda+\mu)}.$$

Constants for Eq. (24) and (25),

$$q_1 = \frac{\delta_4\delta_9 - \delta_3\delta_{10}}{\Delta}, \qquad q_2 = \frac{\delta_1\delta_{10} - \delta_2\delta_9}{\Delta}, \qquad q_3 = \frac{\delta_4\delta_{11} - \delta_3\delta_{12}}{\Delta},$$

$$q_4 = \frac{\delta_2 \delta_{11} - \delta_1 \delta_{12}}{\Delta}, \quad q_5 = \frac{\delta_4 \delta_{13} - \delta_3 \delta_{14}}{\Delta}, \quad q_6 = \frac{\delta_1 \delta_{14} - \delta_2 \delta_{13}}{\Delta},$$

$$\delta_9 = \gamma_1^A \kappa_1^A - \frac{\gamma_1^A}{\mathrm{Im}\{\gamma_2^A\}} \mathrm{Im}\{\kappa_2^A \gamma_2^A\},$$

$$\delta_{10} = \mathrm{Re}\{\kappa_2^A \gamma_2^A\} - \frac{\mathrm{Re}\{\gamma_2^A\}}{\mathrm{Im}\{\gamma_2^A\}} \mathrm{Im}\{\kappa_2^A \gamma_2^A\},$$

$$\delta_{11} = -\alpha_1^A \kappa_1^A - \beta_1^A + \frac{\gamma_1^A}{\mathrm{Im}\{\gamma_2^A\}} \mathrm{Im}\{\kappa_2^A \alpha_2^A + \beta_2^A\},$$

$$\delta_{12} = -\mathrm{Re}\{\kappa_2^A \alpha_2^A + \beta_2^A\} + \frac{\mathrm{Re}\{\gamma_2^A\}}{\mathrm{Im}\{\gamma_2^A\}} \mathrm{Im}\{\kappa_2^A \alpha_2^A + \beta_2^A\},$$

$$\delta_{13} = e_{31}\left(\alpha_1^A - \mathrm{Im}\{\alpha_2^A\}\frac{\gamma_1^A}{\mathrm{Im}\{\gamma_2^A\}}\right) + e_{33}\left[-\beta_1^A \kappa_1^A + \frac{\gamma_1^A}{\mathrm{Im}\{\gamma_2^A\}}\mathrm{Im}\{\kappa_2^A \beta_2^A\}\right] + \in_{33}^\varepsilon \delta_9,$$

$$\delta_{14} = e_{31}\left(\mathrm{Re}\{\alpha_2^A\} - \mathrm{Im}\{\alpha_2^A\}\frac{\mathrm{Re}\{\gamma_2^A\}}{\mathrm{Im}\{\gamma_2^A\}}\right) + e_{33}\left[-\mathrm{Re}\{\kappa_2^A \beta_2^A\} + \frac{\mathrm{Re}\{\gamma_2^A\}}{\mathrm{Im}\{\gamma_2^A\}}\mathrm{Im}\{\kappa_2^A \beta_2^A\}\right] + \in_{33}^\varepsilon \delta_{10}.$$

Appendix E

Equation (14a) can be reformulated as

$$\begin{cases} \sqrt{\dfrac{2}{\pi}} \displaystyle\int_0^\infty \left[\delta_1 L^A(p) + \delta_2\,\mathrm{Re}\{M^A(p)\}\right] p\sin(px)\mathrm{d}p = \sigma_{xy}(x,0) \\[2mm] \sqrt{\dfrac{2}{\pi}} \displaystyle\int_0^\infty \left[\delta_3 L^A(p) + \delta_4\,\mathrm{Re}\{M^A(p)\}\right] p\cos(px)\mathrm{d}p = \sigma_{yy}(x,0) \end{cases} \qquad |x| < \infty \qquad (\text{E1})$$

Making use of the following integrals

$$\begin{cases} \displaystyle\int_0^\infty \sin(pt)\cos(px)\mathrm{d}p = \dfrac{t}{t^2 - x^2} \\[2mm] \dfrac{2}{\pi}\displaystyle\int_0^\infty \sin(pt)\sin(px)\mathrm{d}p = \dfrac{2}{\pi}\displaystyle\int_0^\infty \cos(pt)\cos(px)\mathrm{d}p = \delta(x - t) \end{cases}, \qquad (\text{E2})$$

and noting that

$$\sigma_{xy}(x, 0) = \frac{2}{\pi} \int_0^a \sigma_{xy}(t, 0) \int_0^\infty \sin(px)\sin(pt)\mathrm{d}p\,\mathrm{d}t$$

$$\sigma_{yy}(x, 0) = \frac{2}{\pi} \int_0^a \sigma_{yy}(t, 0) \int_0^\infty \cos(px)\cos(pt)\mathrm{d}p\,\mathrm{d}t$$

(E3)

Equation (14b) can be changed to

$$-\frac{2}{\pi} g_3 \int_0^a \sigma_{yy}(t, 0)\frac{x\,\mathrm{d}t}{t^2 - x^2} + g_4 \sigma_{xy}(x, 0) = 0$$

(E4)

$$g_1 \sigma_{yy}(x, 0) + \frac{2}{\pi} g_2 \int_0^a \sigma_{xy}(t, 0)\frac{t\,\mathrm{d}t}{t^2 - x^2} = d_{31} E_0$$

(E5)

where

$$g_1 = \frac{\delta_2 \delta_7 - \delta_1 \delta_8}{\Delta}, \qquad g_2 = \frac{\delta_3 \delta_8 - \delta_4 \delta_7}{\Delta},$$

$$g_3 = \frac{\delta_2 \delta_5 - \delta_1 \delta_6}{\Delta}, \qquad g_4 = \frac{\delta_3 \delta_6 - \delta_4 \delta_5}{\Delta}, \qquad \Delta = \delta_1 \delta_4 - \delta_2 \delta_3$$

Since $\sigma_{yy}(-t, 0) = \sigma_{yy}(t, 0)$ and $\sigma_{xy}(-t, 0) = -\sigma_{xy}(t, 0)$, it can be proved that

$$2\int_0^a \sigma_{yy}(t, 0)\frac{x\,\mathrm{d}t}{t^2 - x^2} = \int_{-a}^a \frac{\sigma_{yy}(t, 0)\mathrm{d}t}{t - x}, \quad 2\int_0^a \sigma_{xy}(t, 0)\frac{x\,\mathrm{d}t}{t^2 - x^2} = \int_{-a}^a \frac{\sigma_{xy}(t, 0)\mathrm{d}t}{t - x} \quad \text{(E6)}$$

We define $g_0 = \sqrt{\dfrac{g_2 g_4}{g_1 g_3}}$, $g = \dfrac{g_3}{g_4} g_0$ and Eq. (15). Eqs. (E4) and (E5) can then be combined to

obtain Eq. (16).

23

References

Ashley, S., 1995. Smart skis and other adaptive structures. Mech. Eng. 117(11), 76-81.

Beom, H.G. and Atluri S.N., 1996. Near-tip fields and intensity factors for interfacial cracks in dissimilar anisotropic piezoelectric media. Int. J. Fract. 75(2), 163-183.

Broutman, L.J. and Agarwal, B.D., 1974. A theoretical study of the effect of an interfacial layer on the properties of composites. Polym. Eng. Sci. 14(8), 581-588.

Busche, M.J. and Hsia, K.J., 2001. Fracture and domain switching by indentation in barium titanate single crystals. Scripta mater. 44, 207-212.

Carrara, A.S. and McGarry, F.J., 1968. Matrix and interface stresses in a discontinuous fiber composite model. J. Compos. Mater. 2(2), 222-243.

Chopra, I., 1996. Review of current status of smart structures and integrated systems. SPIE-Int. Soc. Opt. Eng. Proceedings of SPIE - the International Society for Optical Engineering 2717, 20-62.

Du, T.B., Liu, M., Seghi, S., Hsia, K.J., Economy, J. and Shang, J.K., 2001. Piezoelectric actuation of crack growth along polymer-metal interfaces in adhesive bonds. J. Mater. Res. 16, 2885-2892.

Erdogan, F., 1965. Stress distribution in bonded dissimilar materials with cracks. J. Appl. Mech. 32, 403-410.

Fotinich, Y. and Carman, G.P., 2000. Stresses in piezoceramics undergoing polarizatioin switching. J. Appl. Phys. 88, 6715-6725.

Fu, R. and Zhang T.Y., 2000. Influence of temperature and electric field on the bending strength of lead zirconate titanate ceramics. Acta Mater. 48, 1729-1740.

Fulton, C.C. and Gao H., 2001. Effect of local polarization switching on piezoelectric fracture. J. Mech. Phys. Solids 49, 927-952.

Furuta, A. and Uchino, K., 1993. Dynamic observation of crack propagation in piezoelectric multilayer ceramic actuators. J. Am. Ceram. Soc. 76, 1615-1617.

Gao, C.F. and Wang, M.Z., 2001. Green's functions of an interfacial crack between two dissimilar piezoelectric media. Int. J. Solids Struct. 38, 5323-5334.

Gao, H., Zhang, T.Y., and Tong, P., 1997. Local and global energy release rates for an electrically yielded crack in a piezoelectric ceramic. J. Mech. Phys. Solids 45, 491-510.

Govorukha V.B. and Loboda, V.V., 2000. Contact zone models for an interface crack in a piezoelectric material. Acta Mech. 140, 233-246.

Heyer, V., Schneider, A., Balke, H., Drescher, J. and Bahr, H.-A., 1998. A fracture criterion for conducting cracks in homogeneous poled piezoelectric PZT-PIC 151 ceramics. Acta Mater. 46, 6615-6622.

Kim, S.J. and Jones, J.D., 1996. Effects of piezo-actuator delamination on the performance of active noise and vibration control system. J. Intel. Mat. Syst. Struct. 7, 668-676.

Kwon, J.H. and Lee, K.Y., 2000. Interface crack between piezoelectric and elastic strips. Arch. Appl. Mech. 70, 707-714.

Muskhelishvili, N.I., 1953. Some basic problems of the mathematical theory of elasticity. P. Noordhoff Ltd., Groningen, Holland. 436-441.

Narita, F. and Shindo, Y., 1998. Layered piezoelectric medium with interface crack under anti-plane shear. Theo. Appl. Fract. Mech. 30, 119-126.

Pak, Y.E., 1992. Linear electro-elastic fracture mechanics of piezoelectric materials. Int. J. Frac. 54, 79-100.

Park, S.B. and Sun, C.T., 1995a. Effect of electric field on fracture of piezoelectric ceramics. Int. J. Frac. 70, 203-216.

Park, S.B. and Sun, C.T., 1995b. Fracture criteria of piezoelectric ceramics. J. Am. Ceram. Soc. 78, 1475-1480.

Parton, V.Z., 1976. Fracture mechanics of piezoelectric materials. Acta Astronautica 3, 671-683.

Rice, J.R., 1988. Elastic fracture concepts for interfacial cracks. J. Appl. Mech. 55, 98-103.

Ru, C., 2000. Electrode-ceramic interfacial cracks in piezoelectric multilayer materials. J. Appl. Mech. 67, 255-261.

Shen, S.P., Kuang, Z.B. and Hu, S.L., 1999. Interface crack problems of a laminated piezoelectric plate. Eur. J. Mech. A/Solids 18, 219-238.

Sosa, H.A., 1992. On the fracture mechanics of piezoelectric solids. Int. J. Solids Struct. 29, 2613-2622.

Suo, Z., Kuo, C.-M., Barnett, D.M. and Willis, J.R., 1992. Fracture mechanics for piezoelectric ceramics. J. Mech. Phys. Solids 40, 739-765.

Wang, X.D. and Meguid, S.A., 2000. On the electroelastic behavior of a thin piezoelectric actuator attached to an infinite host structure. Int. J. Solids Struct. 37, 3231-3251.

Winzer, S.R., Shankar, N. and Ritter, A., 1989. Designing cofired multilayer electrostrictive actuators for reliability. J. Am. Ceram. Soc. 72, 2246-2257.

Yang, W. and Suo, Z., 1994. Cracking in ceramic actuators caused by electrostriction. J. Mech. Phys. Solids 42, 649-663.

Zhu, T. and Yang, W., 1999. Fatigue crack growth in ferroelectrics driven by cyclic electric loading. J. Mech. Phys. Solids 47, 81-97.

Table 1. Material Constants

PZT			
$C_{11}^E = 1.38 \times 10^{11}$ Pa	$C_{33}^E = 1.29 \times 10^{11}$ Pa		
$C_{12}^E = 8.83 \times 10^{10}$ Pa	$C_{13}^E = 9.39 \times 10^{10}$ Pa	$C_{44}^E = 2.45 \times 10^{10}$ Pa	
$e_{31} = 1.02$ C/m^2	$e_{33} = 30.7$ C/m^2	$e_{15} = 14.0$ C/m^2	
$\in_{11}^\varepsilon = 1.51 \times 10^{-8}$ C/(Vm)	$\in_{33}^\varepsilon = 1.30 \times 10^{-8}$ C/(Vm)		

AL		
$\lambda = C_{13} = 4.53 \times 10^{10}$ Pa	$\mu = C_{44} = 2.33 \times 10^{10}$ Pa	

$\varphi = -yE_0$, $y \to +\infty$

S^A : Piezoelectric

Poling

$\varphi = 0$

y

x

$2a$

S^B : Elastic

(a)

$\varphi = -yE_0$, $y \to +\infty$

S^A : Piezoelectric

Poling

$\varphi = 0$

S^B : Elastic

(b)

+

S^A : Piezoelectric

Poling

$\varphi = 0$

S^B : Elastic

(c)
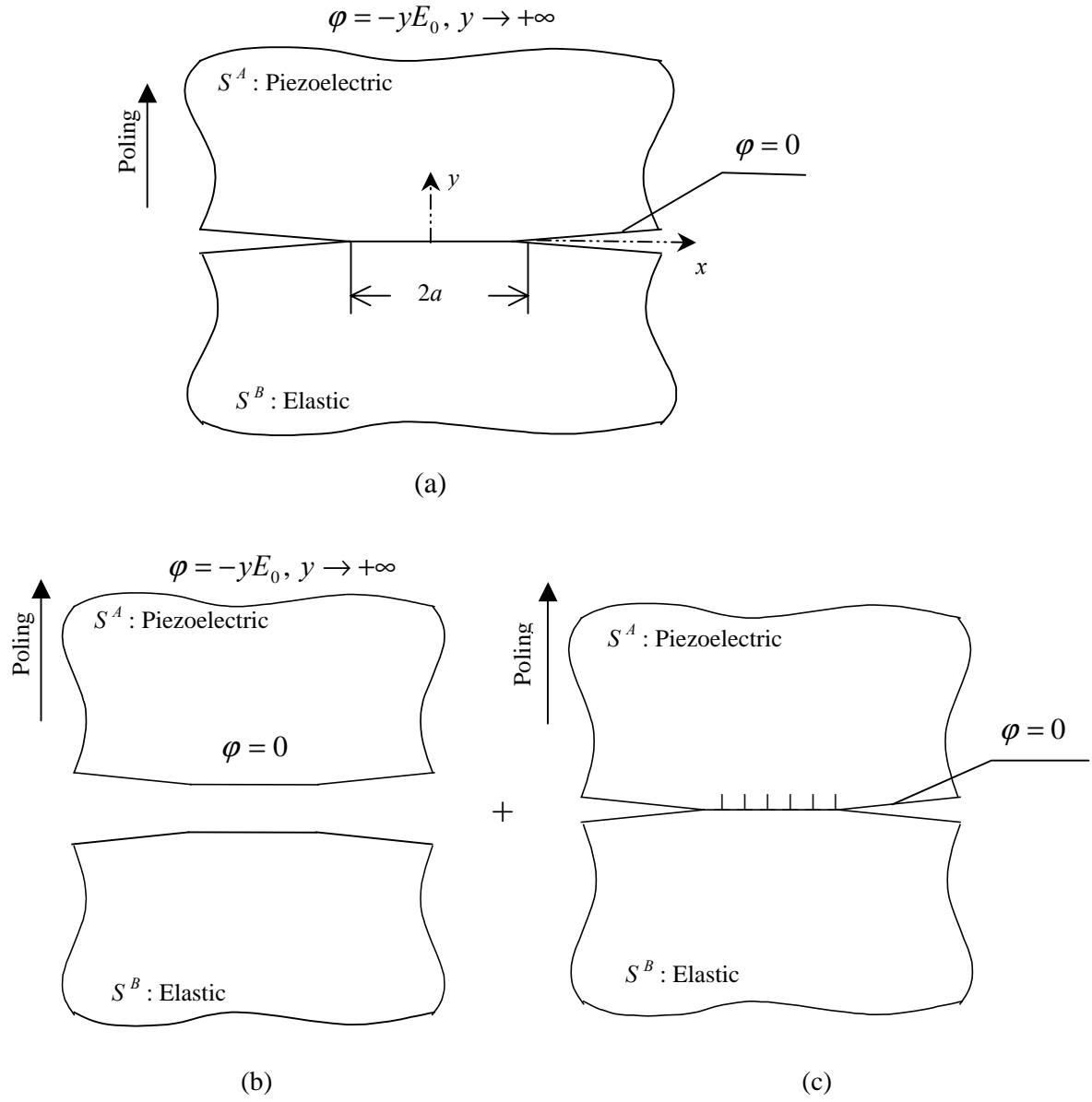
Fig. 1 An interfacial crack between a piezoelectric material and an elastic material under in-plane electric potential loading: (a) configuration to be analyzed; (b) constraint-free body under electric loading; (c) interfacial crack with distributed dislocations.
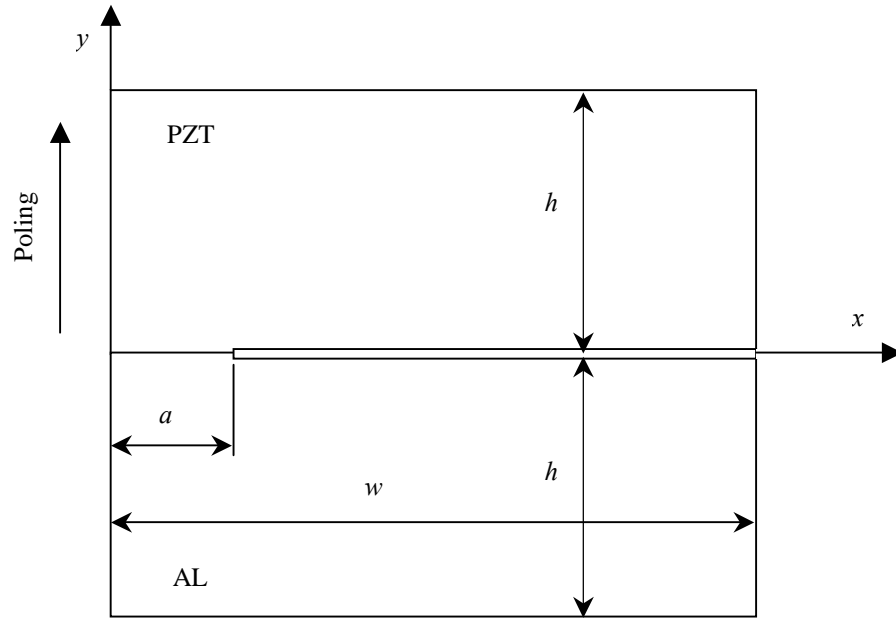
(a)
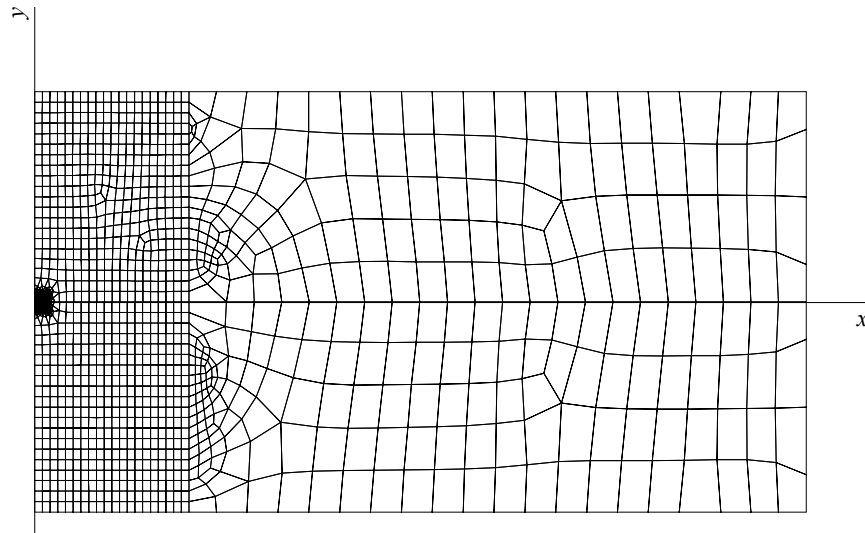
(b)

Fig. 2 (a) Configuration used in the finite element analysis; (b) the finite element mesh.
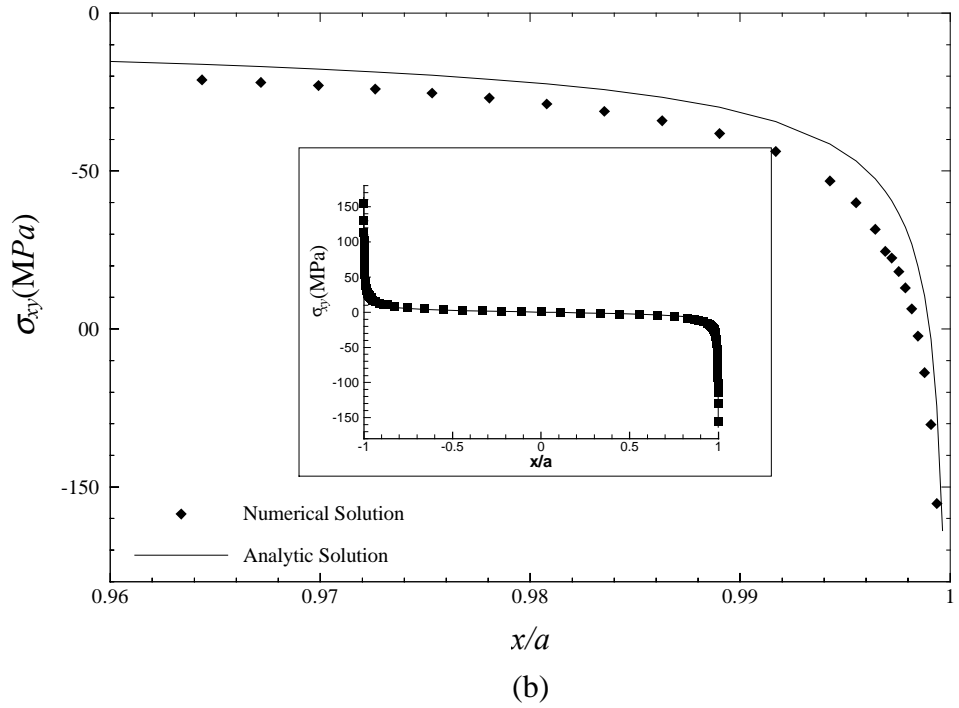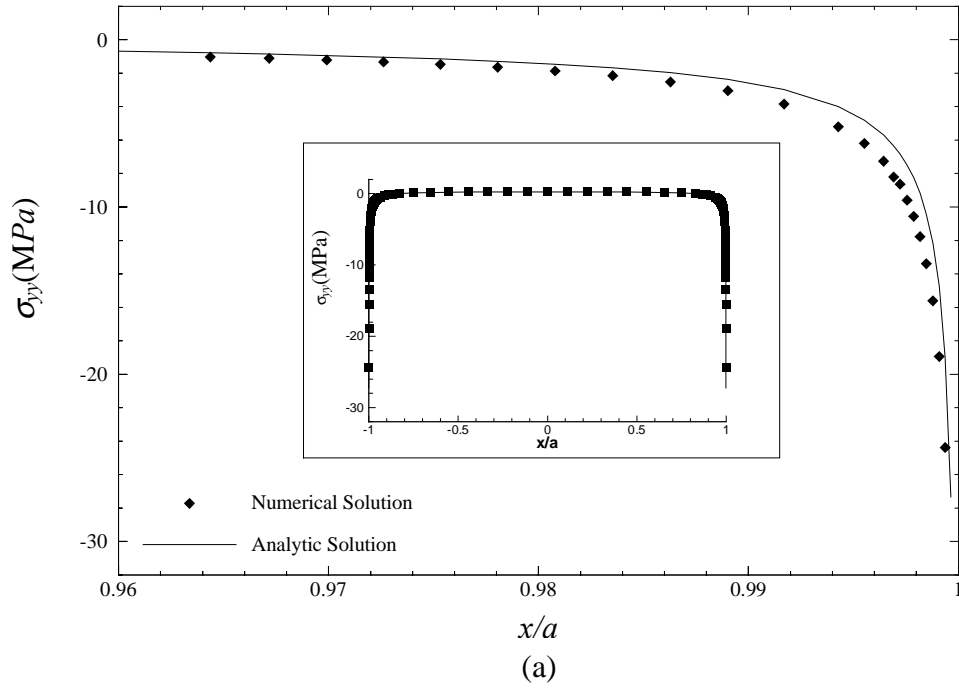
Fig. 3 Stress distribution along the bonded interface: (a) normal stress σ_{yy} distribution; (b) shear stress σ_{xy} distribution.
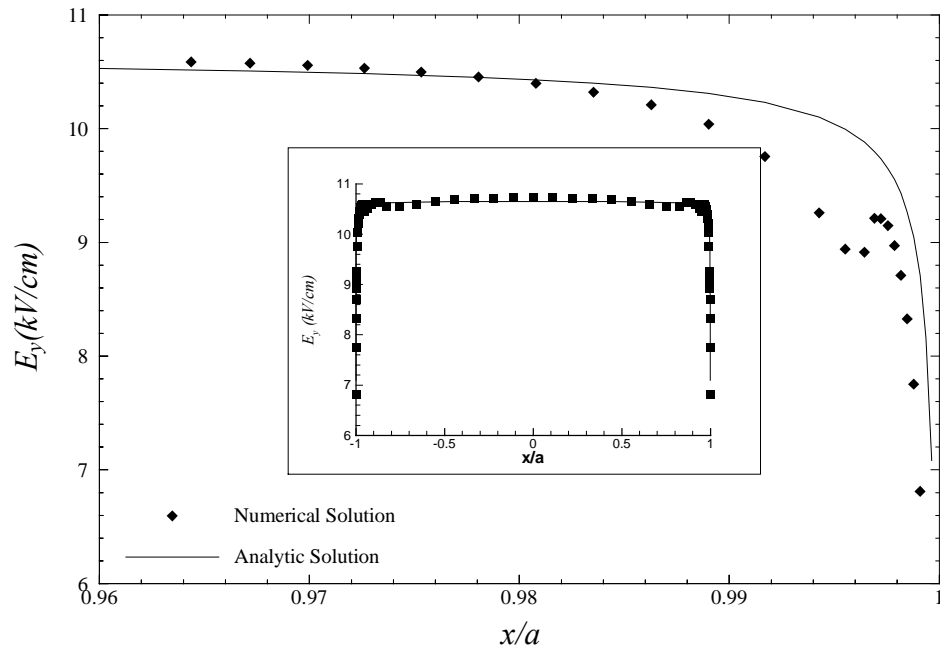
Fig. 4 Distribution of electric field in the poling direction E_y along the bonded interface.
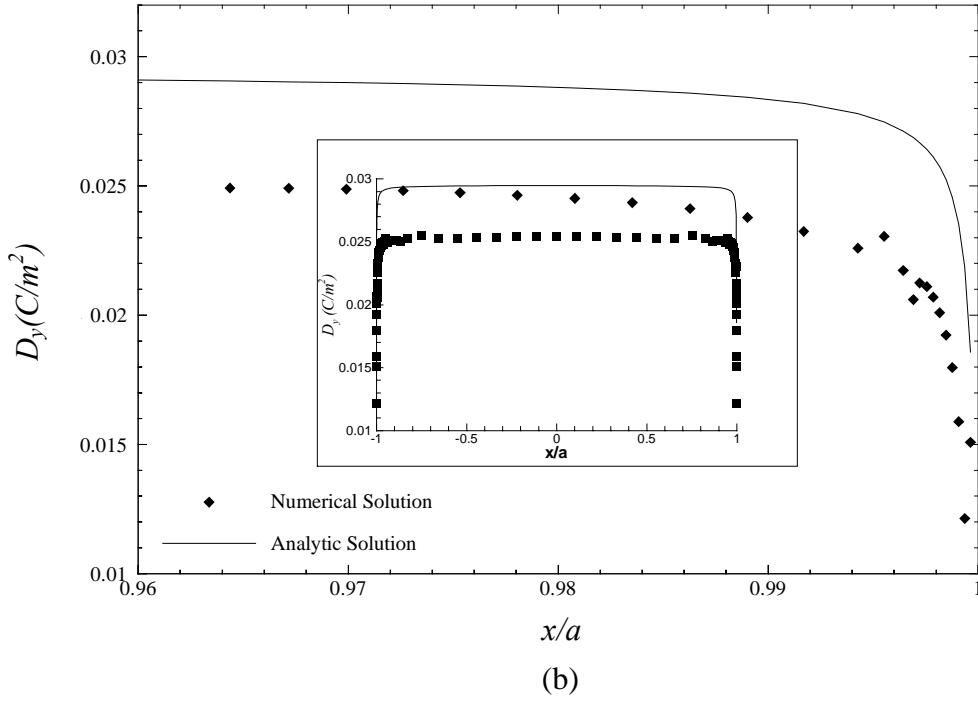
(a)

(b)

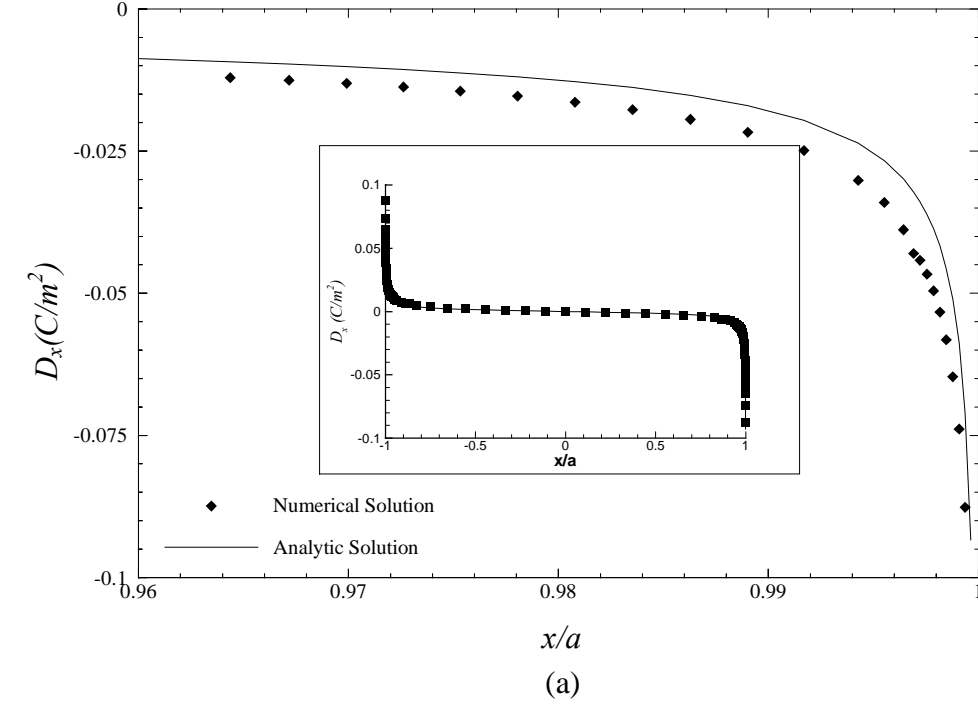Fig. 5 Distributions of Electric displacements along the bonded interface: (a) in *x*-direction D_x; (b) in *y*-direction D_y.